Right-handed neutrino production rate at $T > 160$ GeV

Right-handed neutrino production rate at $T > 160$ **GeV**

I. Ghisoiu[a] and M. Laine[b]

[a]Department of Physics and Helsinki Institute of Physics, University of Helsinki,
P.O.Box 64, FI-00014 Helsinki, Finland

[b]Institute for Theoretical Physics, Albert Einstein Center, University of Bern,
Sidlerstrasse 5, CH-3012 Bern, Switzerland

E-mail: ioan.ghisoiu@helsinki.fi, laine@itp.unibe.ch

Abstract. The production rate of right-handed neutrinos from a Standard Model plasma at a temperature above a hundred GeV has previously been evaluated up to NLO in Standard Model couplings ($g \sim 2/3$) in relativistic ($M \sim \pi T$) and non-relativistic regimes ($M \gg \pi T$), and up to LO in an ultrarelativistic regime ($M \lesssim gT$). The last result necessitates an all-orders resummation of the loop expansion, accounting for multiple soft scatterings of the nearly light-like particles participating in $1 \leftrightarrow 2$ reactions. In this paper we suggest how the regimes can be interpolated into a result applicable for any right-handed neutrino mass and at all temperatures above 160 GeV. The results can also be used for determining the lepton number washout rate in models containing right-handed neutrinos. Numerical results are given in a tabulated form permitting for their incorporation into leptogenesis codes. We note that due to effects from soft Higgs bosons there is a narrow intermediate regime around $M \sim g^{1/2}T$ in which our interpolation is phenomenological and a more precise study would be welcome.

Contents

1 Introduction

The Standard Model completed by several generations of right-handed neutrinos represents a minimal renormalizable framework which is able to describe all available data from terrestrial experiments. It appears well motivated to explore the cosmological significance of this framework [1]–[4]. The present paper aims to contribute to such an endeavour, by studying the behaviour of right-handed neutrinos of any mass M ($1\,\mathrm{GeV} \lesssim M \lesssim 10^{15}\,\mathrm{GeV}$). We concentrate on temperatures above about $160\,\mathrm{GeV}$, so that the Higgs mechanism is not operative and the vacuum masses of particles such as the top quark or $W^{\pm}, Z^{0}$ bosons can be neglected. The right-handed neutrinos interact with the Standard Model degrees of freedom through Yukawa interactions, which are assumed to be weaker than typical Standard Model interactions (gauge interactions, or Yukawa interactions associated with the top quark). We treat the neutrino Yukawa interactions at leading order, whereas for Standard Model interactions the goal is to explore the magnitude of higher-order corrections as well.

It is well known that relativistic thermal field theories suffer from a breakdown of the conventional loop expansion. One reason is that multiple interactions in the plasma generate thermal masses for different excitations, thereby forming a system of "quasiparticles" whose kinematics may differ substantially from the vacuum case. Another aspect of the problem is that when a highly energetic particle passes through a plasma, very many interactions take place within the time scale needed for the initial particle to decay or coalesce into another particle. It is a particular goal of the present paper to derive results which in one limit

extrapolate to the validity range of the conventional loop expansion, and in another to a regime where the mentioned thermal effects need to be systematically "resummed".

More precisely, one observable we consider is the production rate of right-handed neutrinos from an initial state in which the Standard Model particles are in equilibrium at a temperature T, whereas the right-handed neutrinos appear with an abundance much smaller than the equilibrium one. There have been several recent studies of this production rate. In the so-called non-relativistic regime [5–7], the conventional loop expansion does apply, with thermal corrections appearing only through small power corrections $\sim \mathcal{O}(T^2/M^2)$ [8]. Alas, the non-relativistic expansion shows convergence only at very low temperatures $T \lesssim M/15$ [9], by which time most of the physics of interest to, say, leptogenesis, has already played its role [10]. A broader "relativistic" regime $T \lesssim M/3$ can also be addressed up to next-to-leading order (NLO), even if only in numerical form [9]. In the relativistic regime the conventional loop expansion is still valid at NLO. Increasing the temperature to $T \sim M/g^{1/2}$, where g denotes a generic Standard Model coupling, the loop expansion breaks down for the first time. This initial breakdown can be cured by resumming a subset of higher order diagrams into a thermal mass for the Higgs field [9]. Proceeding to $T \gtrsim M/g$, a further reorganization is needed. Then an iterated resummation, including Hard Thermal Loop (HTL) resummation for propagators and vertices, and Landau-Pomeranchuk-Migdal (LPM) resummation accounting for multiple soft scatterings, needs to be implemented in order to obtain correct leading-order (LO) results [11, 12]. As is usual with effective descriptions, the LPM result needs to be systematically combined with other (non-resummed) processes contributing at the same order [13]. Borrowing effective field theory language, we refer to the latter step as a "matching computation". In its current implementation the matching computation is *only* valid for the ultrarelativistic temperatures $T \gtrsim M/g$, because it was carried out by setting $M/T = 0$. It is also discomforting that another (phenomenological) implementation of the matching computation led to a much larger production rate [14].

The objective of the present paper is to suggest a smooth interpolation between the relativistic regime $T \lesssim M/3$ and the LPM-resummed ultrarelativistic regime $T \gtrsim M/g$. We present numerical results in a tabulated form which hopefully permits for their practical incorporation into leptogenesis computations.

The plan of this paper is the following. After defining the observables considered in 2, existing NLO computations and LPM resummations are reviewed in sections 3 and 4, respectively. In section 5 the NLO result is dissected into a contribution also appearing as a part of LPM resummation, and a remainder which needs to be added to the LPM result. An important subtlety, stemming from the fact that the NLO computation reviewed in section 3 was carried out with a vanishing (thermal) Higgs mass, is addressed in section 6. All ingredients are put together in section 7, leading to a single result interpolating between different regimes (however the interpolant's parametric accuracy varies from regime to regime). Some conclusions and an outlook are offered in section 8. Four appendices contain details concerning the NLO result, HTL resummation, cancellation of infrared divergences, and choice of parameters.

2   Basic definitions

Denoting by $\mathcal{K} = (k_0, \mathbf{k})$ the four-momentum of on-shell right-handed neutrinos of mass M, so that $k_0 = \sqrt{k^2 + M^2}$ with $k \equiv |\mathbf{k}|$, and by $h_{\nu i}(\bar{\mu})$ a renormalized $\overline{\text{MS}}$ neutrino Yukawa coupling attaching right-handed neutrinos to the left-handed lepton generation $i \in \{1, 2, 3\}$,

the production rate of out-of-equilibrium right-handed neutrinos from an equilibrium plasma at rest can be expressed as

$$\frac{\mathrm{d}N_+(\mathcal{K})}{\mathrm{d}^4\mathcal{X}\mathrm{d}^3\mathbf{k}} = \frac{2n_{\mathrm{F}}(k_0)}{(2\pi)^3 k_0}|h_\nu|^2\,\mathrm{Im}\,\Pi_{\mathrm{R}}(\mathcal{K}) + \mathcal{O}(|h_\nu|^4)\,, \quad |h_\nu|^2 \equiv \sum_{i=1}^{3}|h_{\nu i}(\bar\mu)|^2\,. \tag{2.1}$$

Here n_{F} is the Fermi distribution (similarly, n_{B} denotes a Bose distribution), and the subscript in N_+ indicates that both spin states have been summed together. The retarded correlator Π_{R} can be expressed as an analytic continuation of a corresponding imaginary-time one,

$$\Pi_{\mathrm{E}}(K) \equiv \mathcal{Z}_\nu\,\mathrm{Tr}\left\{i\slashed{K}\int_0^{1/T}\mathrm{d}\tau\int_{\mathbf{x}}e^{iK\cdot X}\left\langle(\tilde\phi^\dagger a_{\mathrm{L}}\ell)(X)\,(\bar\ell\,a_{\mathrm{R}}\tilde\phi)(0)\right\rangle_T\right\}\,, \tag{2.2}$$

as

$$\Pi_{\mathrm{R}}(\mathcal{K}) = \Pi_{\mathrm{E}}(K)|_{k_n\to-i[k_0+i0^+]}\,. \tag{2.3}$$

In these equations, $\mathcal{Z}_\nu$ is a renormalization factor related to the neutrino Yukawa couplings; $K \equiv (k_n, \mathbf{k})$ where k_n denotes a fermionic Matsubara frequency; $X \equiv (\tau, \mathbf{x})$ is a Euclidean space-time coordinate; $\tilde\phi = i\sigma_2\phi^*$ is a Higgs doublet; $a_{\mathrm{L}}, a_{\mathrm{R}}$ are chiral projectors; ℓ is a left-handed lepton doublet; and $\langle\ldots\rangle_T$ denotes an equilibrium expectation value. At NLO, the renormalization factor reads

$$\mathcal{Z}_\nu = 1 + \frac{1}{(4\pi)^2\epsilon}\left[h_t^2 N_{\mathrm{c}} - \frac{3}{4}(g_1^2 + 3g_2^2)\right] + \mathcal{O}(g^4)\,, \tag{2.4}$$

where the space-time dimension has been expressed as $D = 4 - 2\epsilon$; h_t is the renormalized top Yukawa coupling; $N_{\mathrm{c}} \equiv 3$ is the number of colours; and g_1, g_2 are the renormalized hypercharge and weak gauge couplings, respectively. In addition to these couplings, the Higgs self-coupling λ also appears in our results; how these parameters are fixed in terms of physical observables is explained in appendix D. The notation g^2 refers generically to the couplings $h_t^2, g_1^2, g_2^2, \lambda$ which are taken to be parametrically of the same order of magnitude.

The total production rate of right-handed neutrinos reads

$$\frac{\gamma_+(M)}{|h_\nu|^2} = \int_{\mathbf{k}}\frac{2n_{\mathrm{F}}(k_0)}{k_0}\,\mathrm{Im}\,\Pi_{\mathrm{R}}(\mathcal{K}) + \mathcal{O}(|h_\nu|^2)\,, \tag{2.5}$$

where the integration measure is defined as $\int_{\mathbf{k}} \equiv \int\frac{\mathrm{d}^3\mathbf{k}}{(2\pi)^3}$. A closely related quantity determines the lepton number dissipation ("washout") rate in models containing right-handed neutrinos [15]:

$$\mathcal{W}(M) \equiv -\int_{\mathbf{k}}\frac{2n_{\mathrm{F}}'(k_0)}{k_0}\,\mathrm{Im}\,\Pi_{\mathrm{R}}(\mathcal{K})\,. \tag{2.6}$$

As explained in ref. [15], this needs to be combined with a "susceptibility matrix" and a group-theoretic prefactor of $\mathcal{O}(|h_\nu|^2)$ in order to get the complete result for the washout rate.

Rather than the differential rates $\partial_k\gamma_+$ and $\partial_k\mathcal{W}$, we mostly discuss $\mathrm{Im}\,\Pi_{\mathrm{R}}$ in the following. The reason is that, unlike the integrands in eqs. (2.5), (2.6), $\mathrm{Im}\,\Pi_{\mathrm{R}}$ is a Lorentz-invariant quantity in vacuum, i.e. only dependent on $M^2 = \mathcal{K}^2$ at $T \ll M$ (rather than separately on M and k). At a finite temperature this is no longer the case (cf. figure 4(right)), however even then $\mathrm{Im}\,\Pi_{\mathrm{R}}$ turns out to display only a modest dependence on k for fixed M, and therefore allows us to present results in a relatively economic fashion (i.e. as a sparse table).
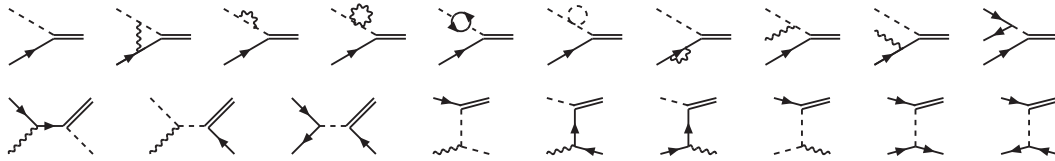
Figure 1. The processes, up to $O(g^2)$, through which right-handed neutrinos can be generated. Arrowed, dashed, and wiggly lines correspond to Standard Model fermions, scalars, and gauge fields, respectively, whereas right-handed neutrinos are denoted by a double line. The closed "virtual" loops include both vacuum and thermal corrections.

3 NLO result in the relativistic regime

We start by discussing the production rate in the "naive" language of Feynman diagrams and the loop expansion. The relevant amplitudes are shown in figure 1. If the right-handed neutrino is massive and all other particles are assumed massless, the LO process is the $2 \to 1$ coalescence depicted up left. The NLO level includes virtual corrections to the $2 \to 1$ reaction, as well as real $3 \to 1$ and $2 \to 2$ processes. In a massless theory, the real and virtual NLO processes are IR divergent; their sum is finite for any $M > 0$ [9, 16]. All the NLO processes have been evaluated numerically in ref. [9].

It was pointed out in ref. [9], however, that for $M \sim g^{1/2}T$ the loop expansion breaks down, and a thermal mass resummation is needed for the Higgs field. The ("asymptotic") thermal masses associated with the Higgs field (m_ϕ) and with left-handed leptons (m_ℓ) are

$$
m_\phi^2 = -\frac{m_H^2}{2} + \left(g_1^2 + 3g_2^2 + \frac{4}{3}h_t^2 N_{\rm c} + 8\lambda\right)\frac{T^2}{16} , \quad m_\ell^2 = \left(g_1^2 + 3g_2^2\right)\frac{T^2}{16} , \qquad (3.1)
$$

where m_H is the vacuum Higgs mass, and corrections of $\mathcal{O}(g^2 m_H^2, g^3 T^2)$ have been omitted [17]. In ref. [9] such a mass resummation was implemented not only for the Higgs field, for which a resummation is unambiguous, but also for leptons, for which it amounts to a higher-order effect when $M \sim g^{1/2}T$. It turns out that once proceeding to $M \lesssim gT$, where thermal mass resummation becomes necessary even for leptons, the correct procedure *differs* from the naive implementation of ref. [9] (the correct procedure for leptons is part of the LPM resummation as discussed in section 4). Hence, in order to be able to combine the NLO result with the LPM result in a systematic way, we need to re-express the NLO result of ref. [9] *without* a thermal mass resummation for leptons.

Keeping a thermal mass for the Higgs only, the leading-order result with a general four-momentum $\mathcal{K}$ in the time-like domain $M^2 \equiv \mathcal{K}^2 > 0$ can be expressed as

$$
{\rm Im}\,\Pi_{\rm R}^{\rm LO} \equiv \frac{(M^2 - m_\phi^2)T}{8\pi k} \ln\left\{ \frac{\sinh\left[\frac{k_+ + m_\phi^2/(4k_+)}{2T}\right] \cosh\left[\frac{k_+(1 - m_\phi^2/M^2)}{2T}\right]}{\sinh\left[\frac{k_- + m_\phi^2/(4k_-)}{2T}\right] \cosh\left[\frac{k_-(1 - m_\phi^2/M^2)}{2T}\right]} \right\} . \qquad (3.2)
$$

Here we have defined

$$
k_\pm \equiv \frac{k_0 \pm k}{2} . \qquad (3.3)
$$

The result of eq. (3.2) can be evaluated (and is positive) both for $M > m_\phi$ and $M < m_\phi$.
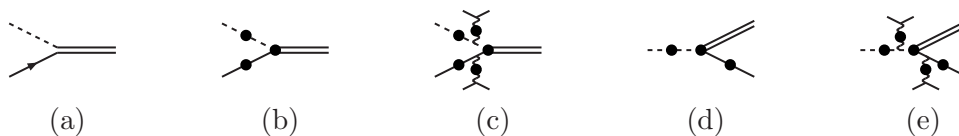
Figure 2. Examples of processes for right-handed neutrino production: (a) a tree-level process producing a massive right-handed neutrino (double line) out of a coalescence of a Higgs (dashed line) and a left-handed lepton (solid line); (b) the same process after HTL resummation, generating thermal self-energies or effective vertices (filled blobs); (c) processes contributing at the same order as (b), due to exchanges of soft $W^\pm, Z^0, \gamma$ bosons; (d) another channel allowed by the thermal masses generated by HTL resummation (if $m_\phi > M$); (e) processes contributing at the same order as (d). In the language of eq. (4.5), the processes (a)–(c) originate from the range $k_0 = \omega_1 + \omega_2$, $\omega_1 > 0$, $\omega_2 > 0$, whereas (d) and (e) correspond to $\omega_2 = k_0 - \omega_1$, $\omega_1 < 0$, where ω_1 is the lepton, ω_2 the Higgs, and k_0 the right-handed neutrino energy.

Once the NLO expression of ref. [9] is written as a sum of eq. (3.2) and a remainder, the final result becomes

$$
\begin{aligned}
\operatorname{Im}\Pi_{\mathrm{R}}^{\mathrm{NLO}} \equiv{}& \operatorname{Im}\Pi_{\mathrm{R}}^{\mathrm{LO}} \\
&+ 2h_t^2 N_{\mathrm{c}}\Bigg\{ -\rho_{\widehat{\mathcal{I}}_{\mathrm{f}}}^T + \rho_{\widehat{\mathcal{I}}_{\mathrm{h}}}^T \\
&\quad - \frac{\pi M^2}{(4\pi)^4 k}\int_{k_-}^{k_+}\mathrm{d}p\,\frac{n_{\mathrm{F}}(k_0-p)n_{\mathrm{B}}(p)}{n_{\mathrm{F}}(k_0)}\left[\ln\frac{(k_+-p)(p-k_-)\bar\mu^2}{k^2 M^2}+\frac{11}{2}\right]\Bigg\} \\
&+ \frac{g_1^2+3g_2^2}{2}\Bigg\{ 2\Big[\rho_{\mathcal{I}_{\mathrm{b}}}^T - \rho_{\widehat{\mathcal{I}}_{\mathrm{b}}}^T + \rho_{\widehat{\mathcal{I}}_{\mathrm{d}}}^T - \rho_{\widehat{\mathcal{I}}_{\mathrm{d}}}^T + \rho_{\mathcal{I}_{\mathrm{g}}}^T + \rho_{\widehat{\mathcal{I}}_{\mathrm{h'}}}^T + \rho_{\mathcal{I}_{\mathrm{j}}}^T\Big] - 4\Big[\rho_{\mathcal{I}_{\mathrm{h}}}^T + \rho_{\widehat{\mathcal{I}}_{\mathrm{h}}}^T\Big] \\
&\quad + \frac{3\pi M^2}{(4\pi)^4 k}\int_{k_-}^{k_+}\mathrm{d}p\,\frac{n_{\mathrm{F}}(k_0-p)n_{\mathrm{B}}(p)}{n_{\mathrm{F}}(k_0)}\left[\ln\frac{(k_+-p)(p-k_-)\bar\mu^2}{k^2 M^2}+\frac{41}{6}\right]\Bigg\}. \quad (3.4)
\end{aligned}
$$

The objects $\rho_{\mathcal{I}_{\mathrm{x}}}^T$ are "master" spectral functions, depending on k_0, k and T and evaluated numerically in refs. [9, 18]. Eq. (3.4) replaces eq. (3.14) of ref. [9]. It should be noted that $m_\phi = 0$ in the terms shown in eq. (3.4), which will play a role in the following (cf. section 6).

Let us reiterate that even though expressed in a concise form in eq. (3.4), the NLO expression incorporates many types of physical processes. There are real $2 \to 2$ and $3 \to 1$ reactions that can be assembled into compact expressions, given in appendix A, which could also have been derived from a Boltzmann equation. In addition there are "virtual" corrections, i.e. self-energy and vertex insertions into the $2 \to 1$ process, given in appendix B. These can be pictured as in figure 2, and include thermal effects represented through the HTL effective theory [19, 20] (actually the HTL vertex correction vanishes). In the NLO computation the self-energy corrections appear as insertions rather than in a fully resummed form, but they nevertheless suffice to cancel soft divergences from the real processes.

4 LPM resummation for light-cone kinematics

When $M \ll \pi T$, all particles participating in $2 \to 1$ processes would be essentially "massless" from the point of view of the thermal motion characterized by the scale πT, were it not that

they obtain effective thermal masses $\sim gT$ through interactions with the other particles in the plasma (the thermal mass of the right-handed neutrino is $\sim |h_\nu|T$ and can be neglected for $|h_\nu| \ll 1$). Typical processes taking place in this situation are depicted in figure 2. Instead of $2 \to 1$ coalescence, $1 \to 2$ decays of thermal Higgs quasiparticles are the dominant "tree-level" process if $gT \gg M$. In addition, however, there are higher-order scatterings, such as those shown in figures 2(c) and 2(e), which are not suppressed despite the additional vertices, because the exchanged t-channel gauge boson has soft virtuality $\sim g^2 T^2$ (it is space-like, and regulated by HTL self-energies). All these processes need to be summed together, which can be achieved through a procedure known as LPM-resummation.

Given that the "leading" particles participating in the reaction are ultrarelativistic, the kinematics of the process amounts to an expansion around the light cone ($k_0 \to k$). Technically this means that kinematic variables are evaluated as a power series in mass/energy, so that for instance $k_0 - k \approx M^2/(2k_0)$. For any fixed M, this implies that only momenta $k \gg M$ are treated consistently. However, in practice the breakdown of the framework does not appear to be dramatic even when this inequality is not strictly satisfied [21].

Following ref. [12] but changing the notation slightly, the basic equations for the LPM resummation can be expressed as follows. Let us define a Hamiltonian

$$\hat{H} \equiv -\frac{M^2}{2k_0} + \frac{m_\ell^2 - \nabla_\perp^2}{2\omega_1} + \frac{m_\phi^2 - \nabla_\perp^2}{2\omega_2} + i\,V(y) \quad y \equiv |\mathbf{y}| \equiv |\mathbf{y}_\perp| \,, \tag{4.1}$$

where $\nabla_\perp$ is a two-dimensional gradient operating in directions orthogonal to $\mathbf{k}$ ($\mathbf{y}_\perp \cdot \mathbf{k} = 0$), and m_ℓ, m_ϕ are the thermal masses from eq. (3.1).[1] The "potential" V plays the role of a "thermal width", erasing phase coherence from a (ϕ, ℓ) pair as it propagates through the plasma; its form reads

$$V(y) = \frac{T}{8\pi} \sum_{i=1}^{2} d_i\, g_i^2 \left[\ln\left(\frac{m_{\mathrm{D}i}\,y}{2}\right) + \gamma_{\mathrm{E}} + K_0\big(m_{\mathrm{D}i}\,y\big) \right] \,, \tag{4.2}$$

where $d_1 \equiv 1$; $d_2 \equiv 3$; K_0 is a Bessel function; and m_{D1}, m_{D2} are electric screening masses for the U(1) and SU(2) gauge bosons:

$$m_{\mathrm{D1}}^2 = \frac{11}{6} g_1^2 T^2 \,, \quad m_{\mathrm{D2}}^2 = \frac{11}{6} g_2^2 T^2 \,. \tag{4.3}$$

With the Hamiltonian at hand, we need to solve the inhomogeneous equations

$$(\hat{H} + i0^+)\,g(\mathbf{y}) = \delta^{(2)}(\mathbf{y}) \,, \quad (\hat{H} + i0^+)\,\mathbf{f}(\mathbf{y}) = -\nabla_\perp \delta^{(2)}(\mathbf{y}) \,. \tag{4.4}$$

Then the LPM-resummed contribution to the correlator of eqs. (2.2), (2.3) reads [12]

$$\mathrm{Im}\,\Pi_{\mathrm{R}}^{\mathrm{LPM}} \equiv -\frac{1}{4\pi} \int_{-\infty}^{\infty} \mathrm{d}\omega_1 \int_{-\infty}^{\infty} \mathrm{d}\omega_2\, \delta(k_0 - \omega_1 - \omega_2) \left[1 - n_{\mathrm{F}}(\omega_1) + n_{\mathrm{B}}(\omega_2) \right]$$

$$\times \frac{k_0}{\omega_2} \lim_{\mathbf{y} \to \mathbf{0}} \left\{ \frac{M^2}{k_0^2} \mathrm{Im}\left[g(\mathbf{y}) \right] + \frac{1}{\omega_1^2} \mathrm{Im}\left[\nabla_\perp \cdot \mathbf{f}(\mathbf{y}) \right] \right\} \,. \tag{4.5}$$

Apart from the LPM result, hard $2 \to 2$ scatterings also contribute in the ultrarelativistic regime [13]. In our approach these originate from the part of the NLO result (section 3)

---

[1]The overall sign of iV is a convention and can be reversed by a corresponding sign change in eq. (4.5).

which is left over when the resummed $1 + n \leftrightarrow 2 + n$ processes, now part of the LPM expression, are subtracted. This subtraction is accomplished in section 5.

As has been discussed in ref. [21] (following a strategy originally proposed in ref. [22]), the solutions of the inhomogeneous equations (4.4) can be reduced to regular solutions (u_ℓ^r) of the corresponding homogeneous equations, with a specific angular quantum number (denoted by $\ell \in \mathbb{Z}$). Introducing a dimensionless variable $\rho \equiv y\, m_{\mathrm{D2}}$, the homogeneous equation reads

$$\left[-\frac{\mathrm{d}^2}{\mathrm{d}\rho^2} + \frac{\ell^2 - 1/4}{\rho^2} + \frac{M_{\mathrm{eff}}^2(\omega)}{m_{\mathrm{D2}}^2} + 2i\, \frac{\omega(k_0 - \omega)}{k_0 m_{\mathrm{D2}}^2} V\!\left(\frac{\rho}{m_{\mathrm{D2}}}\right) \right] u_\ell^r(\rho) = 0 \,, \qquad (4.6)$$

where the particle masses appear through the combination

$$M_{\mathrm{eff}}^2(\omega) \equiv \frac{(k_0 - \omega)m_\ell^2}{k_0} + \frac{\omega m_\phi^2}{k_0} - \frac{\omega(k_0 - \omega)M^2}{k_0^2} \,. \qquad (4.7)$$

Choosing normalization such that the small-ρ asymptotics reads

$$u_\ell^r(\rho) = \rho^{1/2 + |\ell|} \left[1 + \mathcal{O}(\rho^2) \right] \,, \qquad (4.8)$$

eq. (4.5) can then be re-written as

$$\begin{aligned} \mathrm{Im}\,\Pi_{\mathrm{R}}^{\mathrm{LPM}} = -\frac{1}{\pi^2} \int_{-\infty}^{\infty} \mathrm{d}\omega \left[1 - n_{\mathrm{F}}(\omega) + n_{\mathrm{B}}(k_0 - \omega) \right] \\ \times \int_0^\infty \mathrm{d}\rho \left[\frac{\omega M^2}{4k_0^2} \mathrm{Im}\!\left\{ \frac{1}{[u_0^r(\rho)]^2} \right\} + \frac{m_{\mathrm{D2}}^2}{\omega} \mathrm{Im}\!\left\{ \frac{1}{[u_1^r(\rho)]^2} \right\} \right] . \end{aligned} \qquad (4.9)$$

We have checked numerically that this agrees with the results of ref. [12].

5 Subtraction of a $2 \leftrightarrow 1$ part from the NLO expression

The NLO expression of section 3 contains $2 \to 1$, $2 \to 2$, and $3 \to 1$ processes (cf. appendix A). The LPM resummation of section 4 treats $2 + n \leftrightarrow 1 + n$ processes to all orders. However, it does nothing to $2 \to 2$ and $3 \to 1$ processes. Therefore, the $2 \to 2$ and $3 \to 1$ processes of the NLO expression need to be added to the LPM result [13]. But in order to avoid double counting in doing so, the $2 \to 1$ part needs first to be subtracted from the NLO expression.

Of course, the $2 \to 1$ part cannot be subtracted from the NLO expression as such, because virtual corrections make it infrared divergent. Yet it is only a particular subpart of the virtual corrections to the $2 \to 1$ processes, given by HTL effects, which play a role in the LPM resummation. It turns out that if we carry out HTL resummation also in the real $2 \to 2$ processes dominated by soft momentum transfer, then the $2 \to 1$ and $2 \to 2$ processes are *separately* infrared finite. Then we can subtract the HTL-induced $2 \to 1$ part from the NLO expression, and add the remainder to the LPM result.

It is important to note that since in the NLO part of eq. (3.4) all internal particles are massless, we need to set $m_\phi \to 0$ in the corresponding terms of the present section. This does not lead to any divergences, however there is a certain endpoint sensitivity related to Bose-enhanced Higgs bosons which needs to be treated with care (cf. section 6).[2]

---

[2]A different logic for determining the subtraction term was presented for the case of dilepton production from hot QCD in ref. [21]. Applying the same logic here would reproduce eq. (5.9), apart from the term T/k_0, whose sign depends on the ordering of taking $m_\phi/M \to 0$ and $M/k \to 0$ in terms of $\mathcal{O}(m_\ell^2)$.

We proceed in steps. First, the $2 \to 2$ corrections need to be modified such that soft momentum transfer is regulated by HTL resummation. In the NLO expression of section 3, all the correct HTL structures do appear, albeit as "insertions" rather than in a resummed form. As is shown in appendix C (cf. eq. (C.8)), this means that the soft contribution to $2 \to 2$ processes appears as

$$\operatorname{Im} \Pi_{\mathrm{R}}^{\mathrm{HTL,ins,cut}} \equiv \frac{m_\ell^2}{4\pi} \left[n_{\mathrm{B}}(k_0) + \frac{1}{2} \right] \left(\ln \frac{2\Lambda}{\lambda} - 1 \right) , \qquad (5.1)$$

where Λ is an ultraviolet cutoff ($gT \ll \Lambda \ll \pi T$) and λ is an infrared regulator. If the same processes are treated with full HTL resummation, the result gets modified into (cf. eq. (C.6))

$$\operatorname{Im} \Pi_{\mathrm{R}}^{\mathrm{HTL,full,cut}} \equiv \frac{m_\ell^2}{4\pi} \left[n_{\mathrm{B}}(k_0) + \frac{1}{2} \right] \left(\ln \frac{2\Lambda}{m_\ell} - 1 \right) . \qquad (5.2)$$

These results will be needed presently.

Consider then the $2 \to 1$ part of the NLO expression (cf. appendix B). Carrying out the velocity integral as well as the integral over the angles between $\mathbf{p}$ and $\mathbf{k}$ in eq. (B.9), and taking the infrared regulator $\lambda \to 0$ wherever possible, eq. (B.9) can be expressed as

$$\operatorname{Im} \Pi_{\mathrm{R}}^{\mathrm{HTL,ins,pole}} \equiv \frac{1}{8\pi k} \int_{k_- - \frac{m_\ell^2}{4k_-}}^{k_+ - \frac{m_\ell^2}{4k_+}} \frac{\mathrm{d}p\, p}{\epsilon_\ell} (M^2 + m_\ell^2) \left[1 - n_{\mathrm{F}}(\epsilon_\ell) + n_{\mathrm{B}}(k_0 - \epsilon_\ell) \right]$$
$$+ \frac{m_\ell^2}{8\pi k} \int_{k_-}^{k_+} \mathrm{d}p \left[-\frac{k_0}{p} + \frac{M^2}{2p^2} \left(1 - \ln \frac{2p}{\lambda} \right) \right] \left[1 - n_{\mathrm{F}}(p) + n_{\mathrm{B}}(k_0 - p) \right] . \quad (5.3)$$

Here $\epsilon_\ell \equiv \sqrt{p^2 + m_\ell^2}$ and it is understood that we expand to $\mathcal{O}(m_\ell^2)$ after the computation. The integration ranges in eq. (5.3) originate from $\delta(k_0 - \epsilon_\ell - |\mathbf{p} - \mathbf{k}|)$ in the terms where the next-to-leading order in m_ℓ^2 is needed, and from $\delta(k_0 - p - |\mathbf{p} - \mathbf{k}|)$ otherwise.

The first line of eq. (5.3) is readily integrated by taking ϵ_ℓ as an integration variable. Expanding subsequently in m_ℓ^2 and taking also the limit $M \ll k$ leads to

$$\delta_1 \operatorname{Im} \Pi_{\mathrm{R}}^{\mathrm{HTL,ins,pole}} \equiv \frac{m_\ell^2}{8\pi} \left\{ \frac{T}{k_0} + \int_0^{k_0} \frac{\mathrm{d}\omega}{k_0} \left[n_{\mathrm{B}}(k_0 - \omega) - n_{\mathrm{B}}(k_0) - n_{\mathrm{F}}(\omega) + n_{\mathrm{F}}(0) \right] \right\} , \qquad (5.4)$$

where the term of $\mathcal{O}(m_\ell^0)$ was omitted (it will be added separately later on). In order to integrate the term $-k_0/p$ on the second line of eq. (5.3), we add and subtract the value of $1 - n_{\mathrm{F}}(p) + n_{\mathrm{B}}(k_0 - p)$ at $p = 0$ and take subsequently $M \ll k$, producing

$$\delta_2 \operatorname{Im} \Pi_{\mathrm{R}}^{\mathrm{HTL,ins,pole}} \equiv \frac{m_\ell^2}{8\pi} \left\{ \left[n_{\mathrm{B}}(k_0) + \frac{1}{2} \right] \ln\left(\frac{M^2}{4k_0^2} \right) \right.$$
$$\left. - \int_0^{k_0} \frac{\mathrm{d}\omega}{\omega} \left[n_{\mathrm{B}}(k_0 - \omega) - n_{\mathrm{B}}(k_0) - n_{\mathrm{F}}(\omega) + n_{\mathrm{F}}(0) \right] \right\} . \qquad (5.5)$$

For the last part of eq. (5.3), we carry out a similar addition-subtraction step, and note that with the subtracted weight, the integral is only logarithmically sensitive to the lower bound. This yields a contribution of $\mathcal{O}((m_\ell^2 M^2/k_0^2) \ln^2(M^2/2\lambda k_0)) \sim \mathcal{O}(g^4 T^2)$ which is omitted from the HTL consideration (the logarithmic divergence cancels against real corrections). The other part is easily integrated, and a substitution at the lower bound gives

$$\delta_3 \operatorname{Im} \Pi_{\mathrm{R}}^{\mathrm{HTL,ins,pole}} \equiv \frac{m_\ell^2}{8\pi} \left[n_{\mathrm{B}}(k_0) + \frac{1}{2} \right] \ln\left(\frac{4\lambda^2 k_0^2}{M^4} \right) . \qquad (5.6)$$

We can now define the HTL-induced $2 \to 1$ part of the NLO result. We write this as

$$\operatorname{Im} \Pi_{\mathrm{R}}^{\Delta(2 \to 1)} \equiv \operatorname{Im} \Pi_{\mathrm{R}}^{\Delta(2 \to 1),m_\ell^0} + \operatorname{Im} \Pi_{\mathrm{R}}^{\Delta(2 \to 1),m_\ell^2} . \tag{5.7}$$

The term of $\mathcal{O}(m_\ell^0)$ was omitted above; it needs to be computed in the presence of $m_\phi > 0$ like eq. (3.2). In fact the result is a limit of eq. (3.2) but for the kinematics $M^2 \ll \min(k_0^2, k_0 m_\phi, k_0 T)$ assumed in the LPM computation:

$$\operatorname{Im} \Pi_{\mathrm{R}}^{\Delta(2 \to 1),m_\ell^0} \equiv \frac{(M^2 - m_\phi^2)T}{8\pi k_0} \ln \left\{ \frac{\sinh\left(\frac{k_0}{2T}\right) \cosh\left[\frac{k_0}{2T}\left(1 - \frac{m_\phi^2}{M^2}\right)\right]}{\sinh\left(\frac{k_0 m_\phi^2}{2TM^2}\right)} \right\} . \tag{5.8}$$

The correction of $\mathcal{O}(m_\ell^2)$, in turn, is a sum of eqs. (5.4)–(5.6) and the cut contribution from eq. (5.1) (reshuffled here from the original $2 \to 2$ corrections), from which the HTL-resummed cut of eq. (5.2) is subtracted (since this should now appear as a part of $2 \to 2$ corrections):

$$\operatorname{Im} \Pi_{\mathrm{R}}^{\Delta(2 \to 1),m_\ell^2} \equiv (\delta_1 + \delta_2 + \delta_3) \operatorname{Im} \Pi_{\mathrm{R}}^{\mathrm{HTL,ins,pole}} + \operatorname{Im} \Pi_{\mathrm{R}}^{\mathrm{HTL,ins,cut}} - \operatorname{Im} \Pi_{\mathrm{R}}^{\mathrm{HTL,full,cut}}$$

$$= \frac{m_\ell^2}{8\pi} \left\{ \left[n_{\mathrm{B}}(k_0) + \frac{1}{2} \right] \ln \left(\frac{m_\ell^2}{M^2} \right) + \frac{T}{k_0} \right.$$

$$\left. + \int_0^{k_0} \mathrm{d}\omega \left(\frac{1}{k_0} - \frac{1}{\omega} \right) \left[n_{\mathrm{B}}(k_0 - \omega) - n_{\mathrm{B}}(k_0) - n_{\mathrm{F}}(\omega) + n_{\mathrm{F}}(0) \right] \right\}. \tag{5.9}$$

Note that both the ultraviolet cutoff Λ and the infrared regulator λ have dropped out here. The expression in eq. (5.9) needs to be subtracted from the NLO computation as will be discussed in more detail in section 7, but before doing so we need to clarify one feature of virtual $2 \to 1$ corrections that goes beyond the HTL limit.

6 Issues related to contributions from soft Higgs bosons

It was mentioned in section 3 that, even though the Higgs mass needs to be thermally resummed when $M \lesssim g^{1/2}T$ as done in the LO result of eq. (3.2), the Higgs mass was kept at zero in the NLO contribution of eq. (3.4). This does not cause the NLO contribution to diverge; nevertheless, as we now argue, its value is not physically correct for $M \ll g^{1/2}T$.

The reason for the problem is that there are parts in the NLO contribution which include two Bose factors. This may lead to an enhancement $\sim T^2/\epsilon_\phi^2$, where ϵ_ϕ is the Higgs energy. If the Higgs were massless, its energy could be as small as $\sim M^2/(4k)$, whereby we may obtain a contribution $\sim 4kT^2/M^2$ from $\int \mathrm{d}\epsilon_\phi$. Therefore, even if there were a prefactor M^2, a finite result could be left over. Such an expression is not correct, however, because in the presence of a mass, $\epsilon_\phi \geq m_\phi$, and there can be no divergence at $M/k \to 0$.

There are only two structures in eq. (3.4) which suffer from this problem, namely the master spectral functions $\rho_{\mathcal{I}_\mathrm{h}}^T$ and $\rho_{\mathcal{I}_\mathrm{j}}^T$ which, according to refs. [9, 18], have a finite limit for $M/T \to 0$ even though they contain no HTL structures. Employing the same notation as in

appendices A and B, their contributions to eq. (3.4) can formally be expressed as

$$
\begin{aligned}
n_{\mathrm{F}}(k_0)&\left(\rho_{\mathcal{I}_{\mathrm{j}}}^T - 2\rho_{\mathcal{I}_{\mathrm{h}}}^T\right) \\
&= \int \mathrm{d}\Omega_{2\to1}\, n_{\mathrm{F}}(p_1)\, n_{\mathrm{B}}(p_2) \mathop{\rlap{\textstyle\sum}\int}_Q \frac{M^2}{Q^2(Q-P_2)^2}\left[1 + \frac{M^2}{(Q-K)^2}\right]\Bigg|_{p_{2n}=-ip_2,\,k_n=-ik_0} \\
&\quad + \int \mathrm{d}\Omega_{2\to2}\left\{ n_{\mathrm{B}}(p_1)\, n_{\mathrm{B}}(p_2)\left[1 - n_{\mathrm{F}}(k_2)\right]\left[-\frac{M^2(M^2-t)}{st}\right]\right. \\
&\qquad\qquad\left. + n_{\mathrm{F}}(p_1)\, n_{\mathrm{B}}(p_2)\left[1 + n_{\mathrm{B}}(k_2)\right]\left[\frac{M^2(M^2-s)}{st} + \frac{M^2(M^2-u)}{ut}\right]\right\} \\
&\quad + \int \mathrm{d}\Omega_{3\to1}\left\{ n_{\mathrm{F}}(p_1)\, n_{\mathrm{B}}(p_2)\, n_{\mathrm{B}}(p_3)\left[\frac{M^2(M^2-s_{12})}{s_{12}s_{23}}\right]\right\}.
\end{aligned}
\tag{6.1}
$$

Let us illustrate the issue with the simplest term, the self-energy correction ($P_2 \equiv (p_{2n}, \mathbf{p}_2)$)

$$
\phi(p_2) \equiv \mathop{\rlap{\textstyle\sum}\int}_Q \frac{1}{Q^2(Q-P_2)^2}\Bigg|_{p_{2n}=-ip_2}.
\tag{6.2}
$$

In naive power counting this would be of $\mathcal{O}(1)$ and contains *no* HTL structures $\sim T^2$ [23]. However, taken literally, $\phi(p_2)$ is infrared divergent. If we insert a regulator, $1/(Q-P_2)^2 \to 1/[(Q-P_2)^2 + \lambda^2]$, and note that the Bose-enhanced singularities at $q=0$ and $q=p_2$ cancel against real corrections (cf. ref. [9], eq. (B.70) ff), the Bose-enhanced part of the result can be written as (away from singular points and after a partial cancellation against real corrections as well as a substitution $q \to q + p_2$ in one of the terms)

$$
\phi(p_2) \simeq \frac{T}{(4\pi)^2 p_2} \int_0^\infty \frac{\mathrm{d}q}{q} \ln\left|\frac{p+q}{p-q}\right| = \frac{T}{32 p_2}.
\tag{6.3}
$$

Since the answer grows only linearly in T, it is not part of HTLs. Inserting the result into the $2 \to 1$ phase space integral yields subsequently

$$
n_{\mathrm{F}}(k_0)\, \delta\rho_{\mathcal{I}_{\mathrm{h}}}^T \simeq -\frac{\pi M^2 T}{32(4\pi)^2 k} \int_{k_-}^{k_+} \frac{\mathrm{d}p_2}{p_2}\, n_{\mathrm{B}}(p_2) n_{\mathrm{F}}(k_0 - p_2) \simeq -\frac{\pi M^2 T^2 n_{\mathrm{F}}(k_0)}{32(4\pi)^2 k\, k_-},
\tag{6.4}
$$

where we only kept the Bose-enhanced contribution from the lower edge of the integration range. Given that $k_- \approx M^2/(4k)$ for $M \ll k$, the factor M^2 is seen to cancel out, leaving over a finite contribution.

This finite contribution is not "correct", however. Indeed, had we had the Higgs mass in the $2 \to 1$ phase space integral, the minimal Higgs energy would have been $\epsilon_\phi^{\min} = k_- + m_\phi^2/(4k_-)$ for $M > m_\phi$, and $\epsilon_\phi^{\min} = k_+ + m_\phi^2/(4k_+)$ for $M < m_\phi$. Obviously $\epsilon_\phi^{\min} \geq m_\phi$ for any M, and to a good approximation $\epsilon_\phi^{\min} \approx k_0$ for $M \lesssim m_\phi$. In $2 \to 2$ scatterings smaller values can appear, but in any case $\epsilon_\phi^{\min} \geq m_\phi$ is always satisfied.

In order to account for these features properly, the NLO computations of refs. [9, 18] should be repeated with $m_\phi > 0$. This is a hard task and goes beyond the scope of the present study. Here, we rather resort to a phenomenological interpolation which has the correct limiting values for $M \gg g^{1/2}T$ and $M \ll g^{1/2}T$.

According to $2 \to 1$ kinematics with $\epsilon_\phi^{\min} = k_- + m_\phi^2/(4k_-)$ for $M > m_\phi$, the phase space employed in the NLO result of eq. (3.4), as illustrated in eq. (6.4), is physically correct

– 10 –

only if $k_- \gg m_\phi^2/(4k_-)$. For $M \ll k$ this corresponds to $m_\phi \ll M^2/(2k)$. We need to "switch off" the incorrect contributions as soon as this inequality is not satisfied. This can be achieved by defining

$$\operatorname{Im}\Pi_{\mathrm{R}}^{\mathrm{NLO},\phi} \equiv \operatorname{Im}\Pi_{\mathrm{R}}^{\mathrm{NLO}} - \Theta\Big(\frac{2km_\phi}{M^2}-1\Big)\big(g_1^2+3g_2^2\big)\big(\rho_{\mathcal{I}_{\mathrm{j}}}^T - 2\rho_{\mathcal{I}_{\mathrm{h}}}^T\big)\,, \qquad (6.5)$$

where Θ is a smoothed step function, for instance $\Theta(x) \equiv [1 + \tanh(2x)]/2$. Obviously, the recipe is purely phenomenological in the intermediate range $M \sim \sqrt{2km_\phi}$, but it does have the correct limiting values on both sides of this range. For illustration of the numerical (un)importance of the precise choice made, we also consider an implementation with another width of the switch-off region, namely

$$\operatorname{Im}\tilde{\Pi}_{\mathrm{R}}^{\mathrm{NLO},\phi} \equiv \operatorname{Im}\Pi_{\mathrm{R}}^{\mathrm{NLO}} - \Theta\Big(\frac{m_\phi^2/4k_- - k_-}{T}\Big)\big(g_1^2+3g_2^2\big)\big(\rho_{\mathcal{I}_{\mathrm{j}}}^T - 2\rho_{\mathcal{I}_{\mathrm{h}}}^T\big)\,. \qquad (6.6)$$

The difference with respect to eq. (6.5) is plotted as a grey band in figures 3(right) and 4(left), and is practically invisible in the final result shown in figure 4(left).

7 Putting together the NLO and LPM results

After the considerations of sections 5 and 6, we are in a position to subtract the HTL-induced $2 \to 1$ part from the NLO expression. The remainder, incorporating HTL-resummed $2 \to 2$ processes, subleading corrections to $2 \to 1$ processes, and $3 \to 1$ processes (which do not contribute when $M/T \to 0$), is defined as

$$\operatorname{Im}\Pi_{\mathrm{R}}^{\Delta(2\to 2)} \equiv \operatorname{Im}\Pi_{\mathrm{R}}^{\mathrm{NLO},\phi} - \operatorname{Im}\Pi_{\mathrm{R}}^{\Delta(2\to 1)}\,, \qquad (7.1)$$

where $\operatorname{Im}\Pi_{\mathrm{R}}^{\mathrm{NLO},\phi}$ is from eq. (6.5) and $\operatorname{Im}\Pi_{\mathrm{R}}^{\Delta(2\to 1)}$ is from eqs. (5.7)–(5.9).

Returning briefly to $\operatorname{Im}\Pi_{\mathrm{R}}^{\Delta(2\to 1)}$, we note that the first term on the right-hand side of eq. (5.9) is logarithmically divergent for $M^2 \to 0$. The divergence also appears in the NLO result, and is removed by the subtraction in eq. (7.1). This cancellation constitutes a crosscheck of our computation. The logarithmic dependence on m_ℓ in eq. (5.9) can also be compared with literature: our result agrees with ref. [13], after noting that $n_{\mathrm{B}}(k_0) + \frac{1}{2}$ can be expressed as $n_{\mathrm{B}}(k_0)/[2n_{\mathrm{F}}(k_0)]$ and that the discussion in ref. [13] concerns the integrand of eq. (2.5).

Having subtracted the $\Delta(2\to 1)$ part, eq. (7.1) can be added to the LPM expression of section 4, which leads to our final result:

$$\operatorname{Im}\Pi_{\mathrm{R}} \equiv \operatorname{Im}\Pi_{\mathrm{R}}^{\mathrm{LPM}} + \operatorname{Im}\Pi_{\mathrm{R}}^{\Delta(2\to 2)}\,. \qquad (7.2)$$

How accurate this expression is, depends on the regime considered: in the relativistic regime $M \gtrsim \pi T$ relative errors are of $\mathcal{O}(g^3)$, whereas in the ultrarelativistic regime $M \lesssim gT$ relative errors are likely to be suppressed by $\mathcal{O}(g)$ [24, 25]. In between there is a regime in which the expression is not consistent even at leading order, as has been discussed in section 6.

Let us proceed to numerical evaluations. In figure 3(left), the "naive" NLO and LPM results from eqs. (6.5) and (4.9) are shown; in figure 3(right), the difference defined by eq. (7.1), which needs to be added to the LPM result, is displayed. The final estimate from eq. (7.2) is shown in figure 4(left) as a function of M/T; and in figure 4(right) as a function
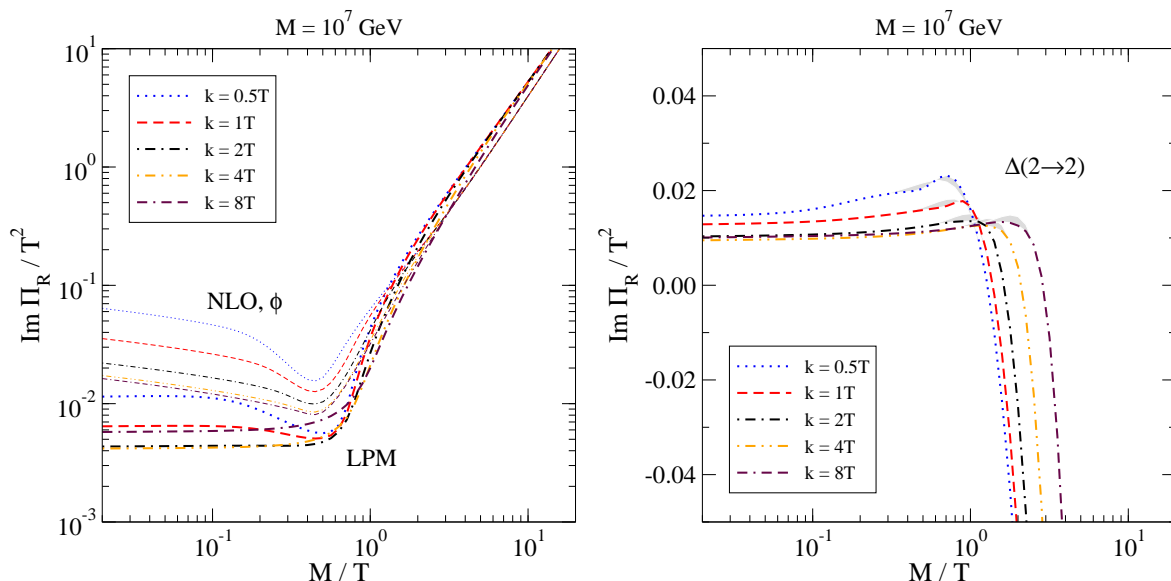
Figure 3. Left: NLO correlator from eq. (6.5) (thin lines) and the LPM one from eq. (4.9) (thick lines). Right: correction of the LPM result through $\Delta(2\rightarrow2)$ from eq. (7.1). The couplings and the renormalization scale are fixed as specified in appendix D.
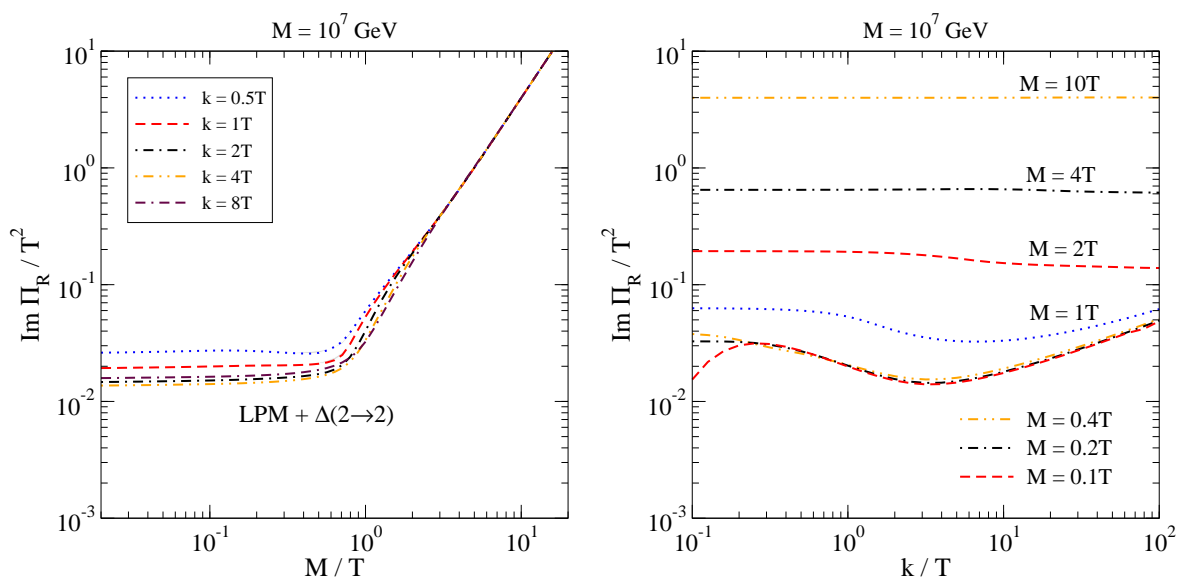

Figure 4. Left: final results for the correlator in eq. (7.2). Right: the same results as a function of k/T. The couplings and the renormalization scale are fixed as specified in appendix D.

of k/T. In figures 3(right) and 4(left), the uncertainty related to the phenomenological step in eq. (6.5) is illustrated with a grey band (cf. the discussion around eq. (6.6)). The total rates, from eqs. (2.5) and (2.6), are shown in figure 5. Finally, in figure 6 we display on a linear scale how the full result is made up of the LPM-resummed $2 \leftrightarrow 1$ result, and $2 \rightarrow 2$ and $3 \rightarrow 1$ scatterings as well as subleading corrections to $2 \leftrightarrow 1$ processes involving top quarks and gauge bosons.
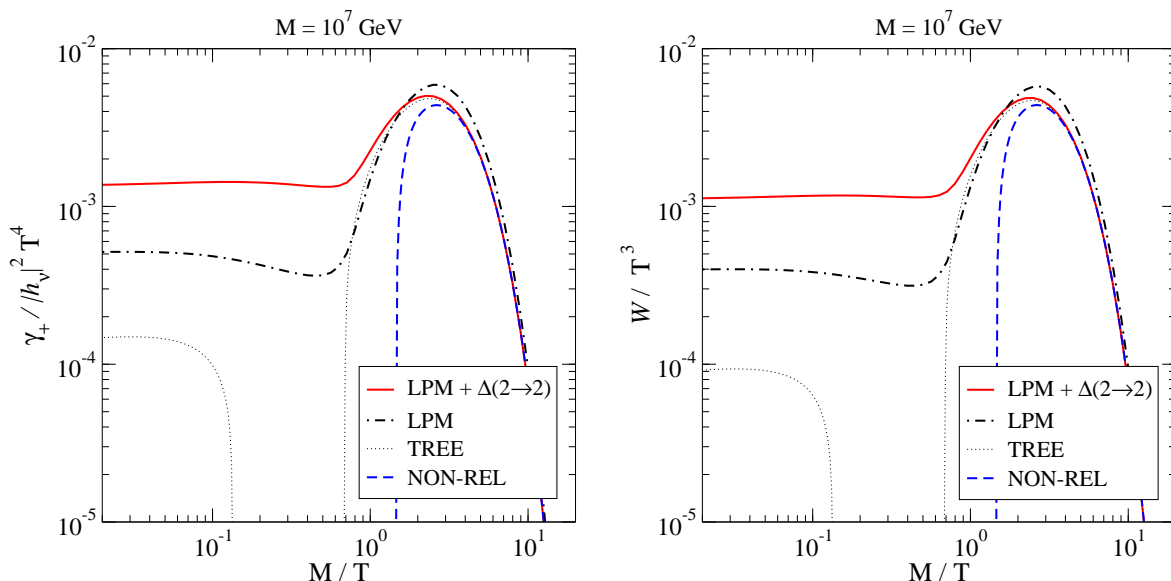
Figure 5. Left: total right-handed neutrino production rate from eq. (2.5), for $M = 10^7$ GeV. Shown are results from eq. (7.2) ("LPM + $\Delta(2 \to 2)$"); eq. (4.9) ("LPM"); with naive thermal masses as given e.g. in eq. (3.9) of ref. [9] ("TREE"); and from ref. [6] ("NON-REL"). Right: similar results for the function defined in eq. (2.6). The solid lines constitute our final results.
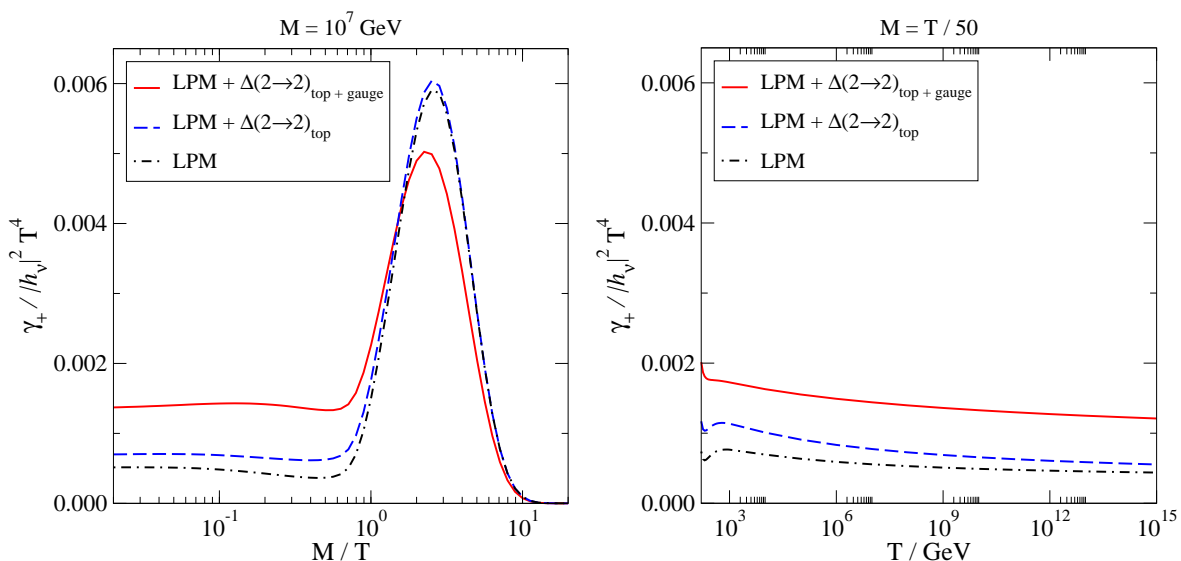

Figure 6. Left: like figure 5(left) but with $\Delta(2 \to 2)$ separated into contributions from top-quark and gauge-boson scatterings. Right: similar results but for fixed $M = 0.02T$, as a function of $T/$GeV.

In addition to the figures, we have prepared a table containing results with temperatures in the range $T = (160 \dots 10^{15})$ GeV, masses in the range $M = (0.02 \dots 20)\, T$, and momenta in the range $k = (10^{-1} \dots 10^2)\, T$. The lowest temperature is determined by the location of the electroweak crossover in the Standard Model [26]. The tabulated results can be downloaded as explained in footnote 3.

A few comments are in order:

- The physical spectra entering eqs. (2.5), (2.6), *viz.*

$$\frac{\partial_k \gamma_+}{|h_\nu|^2} \equiv \frac{k^2 n_{\rm F}(\sqrt{k^2 + M^2})}{\pi^2 \sqrt{k^2 + M^2}} \, {\rm Im}\,\Pi_{\rm R} \,, \tag{7.3}$$

$$\partial_k W \equiv -\frac{k^2 n_{\rm F}'(\sqrt{k^2 + M^2})}{\pi^2 \sqrt{k^2 + M^2}} \, {\rm Im}\,\Pi_{\rm R} \,, \tag{7.4}$$

  can be obtained from the results displayed in figure 4(right) by trivial multiplications.

- Since empirically the results appear to have a smooth limit as $M/T \to 0$ (cf. figure 4(left)), expressions for the massless case $M = 0$ can to a good approximation be obtained from the row of our table having $M = 0.02T$. (Our numerics, optimized for a generic $M \sim T$, becomes ineffective for very small M/T, so we cannot set $M/T = 0$.) Let us note, however, that for $M \lesssim 0.1T$ the spectrum shows an unphysical dip at $k \lesssim 0.2T$, cf. figure 4(right). We believe this to be an artefact of the approximations made, which are based amongst others on the assumption that $k \gg gT$. Fortunately this regime is phase-space suppressed in the observables of figure 5. If however spectral information plays an important role in a particular application, it is probably prudent to use the stable value $M \sim 0.2T$ rather than $M = 0.02T$ as an approximation for $M/T = 0$.

- Typical numerical values of the thermal masses are $m_\phi \sim 0.4T$ and $m_\ell \sim 0.3T$. The rate at $M \ll T$ has a contribution from the $1 \to 2$ decay $\phi \to \ell N$, since $m_\phi > M + m_\ell$ then. At temperatures close to the electroweak crossover, however, the Higgs mass becomes small, cf. eq. (3.1), and another channel may open up. Therefore, the rate has a non-trivial shape at low temperatures, as is visible in figure 6(right).

- For $M \ll T$ our results, as displayed in figures 5 and 6, are in good numerical agreement with ref. [13]. In contrast, the results of ref. [14] are larger by a factor ~ 2. It is difficult to identify a precise reason for the discrepancy, but let us note that if the considerations of section 6 were omitted, i.e. the doubly Bose-enhanced contributions from massless Higgs bosons were included in the NLO expression, our numerical results would be larger by a factor ~ 1.7 at $M \ll T$ (for $M = 10^7$ GeV).

8 Conclusions and outlook

We have provided numerical results for the imaginary part of the right-handed neutrino self-energy, entering gauge-invariant physical observables as dictated by eqs. (2.5) and (2.6), as a function of the right-handed neutrino mass M and momentum k, for a wide range of temperatures $T \geq 160$ GeV.[3] Previous results for $M \ll T$ [13] cannot be extrapolated to $M \gtrsim T$ because the $2 \to 2$ contributions were evaluated by assuming $M/T = 0$, whereas NLO results obtained for $M \gtrsim \pi T$ [9] cannot be extrapolated to $M \ll \pi T$ because of a powerlike breakdown of the loop expansion. Our results smoothly interpolate between the two regimes, although for the moment this comes with the price of a phenomenological treatment in a particular intermediate range (cf. section 6). In order to avoid this compromise in the future,

---

[3]Tabulated results can be downloaded from www.laine.itp.unibe.ch/production-highT/.

the NLO computation of ref. [9] should be repeated with $m_\phi > 0$. From a practical point of view, though, it appears that only a narrow mass range is affected, so that even the present results should suffice for many applications (cf. the grey bands in figures 3(right) and 4(left), the latter being practically invisible).

Apart from numerical evaluations, it would be highly desirable to obtain analytic expressions as well. For the moment this has only been achieved as an expansion in a power series in $(\pi T/M)^2$, corresponding formally to an Operator Product Expansion [8] and referred to as a non-relativistic regime [5–7]. Unfortunately, as discussed in ref. [9], this expansion shows poor convergence for $T \gtrsim M/15$, and is therefore not terribly useful for estimating thermal corrections in practice. Nevertheless it is helpful as a stringent crosscheck passed by the NLO expression [9], as well as a tool for formulating a theoretically consistent framework for the full leptogenesis computation [10].

Let us end by noting that the imaginary part of the right-handed neutrino self-energy has also been studied at temperatures below about $10\,\mathrm{GeV}$ [27].[4] It is a relevant challenge for future work to close the gap between $T \lesssim 10\,\mathrm{GeV}$ and $T \gtrsim 160\,\mathrm{GeV}$.

Acknowledgments

A   Real corrections within the NLO expression

In order to allow for a comparison with Boltzmann equations, we re-write here the "real corrections" appearing in eq. (3.4) in the form of matrix elements squared. The normalization is chosen so as to permit for a direct comparison with the expressions given in table 1 of ref. [13]. (Let us stress again that the $2 \to 2$ and $3 \to 1$ corrections are not integrable as such, but that the expression as a whole is finite, provided that its 1-loop corrected $2 \to 1$ part is added in the presence of a consistent regulator for soft momentum transfer.)

By making use of the results listed in refs. [9, 18], eq. (3.4) can be re-expressed as

$$
\begin{aligned}
2n_{\mathrm{F}}(k_0)\Big[\mathrm{Im}\,\Pi_{\mathrm{R}}^{\mathrm{NLO}} - \mathrm{Im}\,\Pi_{\mathrm{R}}^{\mathrm{LO}}\Big] = &\int \mathrm{d}\Omega_{2\to1}\,\Big\{\text{eq. (B.2)}\Big\} \\
&+ \int \mathrm{d}\Omega_{2\to2}\,\Big\{\, n_{\mathrm{B}}(p_1)\,n_{\mathrm{B}}(p_2)\,\big[1 - n_{\mathrm{F}}(k_2)\big]\,|\mathcal{M}_{\mathrm{a}}|^2 \\
&\qquad\qquad + n_{\mathrm{F}}(p_1)\,n_{\mathrm{B}}(p_2)\,\big[1 + n_{\mathrm{B}}(k_2)\big] \sum |\mathcal{M}_{\mathrm{b}}|^2 \\
&\qquad\qquad + n_{\mathrm{F}}(p_1)\,n_{\mathrm{F}}(p_2)\,\big[1 - n_{\mathrm{F}}(k_2)\big] \sum |\mathcal{M}_{\mathrm{c}}|^2 \,\Big\} \\
&+ \int \mathrm{d}\Omega_{3\to1}\,\Big\{\, n_{\mathrm{F}}(p_1)\,n_{\mathrm{B}}(p_2)\,n_{\mathrm{B}}(p_3)\,|\mathcal{M}_{\mathrm{d}}|^2 \\
&\qquad\qquad + n_{\mathrm{F}}(p_1)\,n_{\mathrm{F}}(p_2)\,n_{\mathrm{F}}(p_3)\,|\mathcal{M}_{\mathrm{e}}|^2 \,\Big\}\,. \qquad (\mathrm{A.1})
\end{aligned}
$$

Here $\mathrm{d}\Omega_{n\to m}$ denotes the usual phase space integration measure with 4-momentum conservation, $\mathrm{d}\Omega_{n\to m} \equiv \Pi_{i=1}^n \frac{\mathrm{d}^3 \mathbf{p}_i}{2p_i(2\pi)^3}\Pi_{j=2}^m \frac{\mathrm{d}^3 \mathbf{k}_j}{2k_j(2\pi)^3}\,(2\pi)^4\,\delta^{(4)}(\sum_{i=1}^n \mathcal{P}_i - \sum_{j=1}^m \mathcal{K}_j)$. The three-momenta of incoming particles are denoted by $\mathbf{p}_i$, with $p_i \equiv |\mathbf{p}_i|$ and $\mathcal{P}_i \equiv (p_i, \mathbf{p}_i)$; those of outgoing

---

[4]Tabulated results can be downloaded from www.laine.itp.unibe.ch/production-lowT/.

particles are $\mathbf{k}_i$, with $\mathbf{k}_1 \equiv \mathbf{k}$ the right-handed neutrino momentum. The matrix elements squared read

$$|\mathcal{M}_{\mathrm{a}}|^2 \equiv (g_1^2 + 3g_2^2)\left(\frac{u - M^2}{t} - \frac{2uM^2}{st}\right), \tag{A.2}$$

$$\sum |\mathcal{M}_{\mathrm{b}}|^2 \equiv (g_1^2 + 3g_2^2)\left(\frac{M^2 - u}{s} + \frac{M^2 - s}{u} + \frac{2uM^2}{st} + \frac{2sM^2}{ut}\right), \tag{A.3}$$

$$\sum |\mathcal{M}_{\mathrm{c}}|^2 \equiv 2h_t^2 N_{\mathrm{c}}\left(3 - \frac{M^2}{s} - \frac{2M^2}{t}\right), \tag{A.4}$$

$$|\mathcal{M}_{\mathrm{d}}|^2 \equiv (g_1^2 + 3g_2^2)\left(\frac{M^2 - s_{13}}{s_{12}} + \frac{2s_{13}M^2}{s_{12}s_{23}}\right), \tag{A.5}$$

$$|\mathcal{M}_{\mathrm{e}}|^2 \equiv 2h_t^2 N_{\mathrm{c}}\left(-1 + \frac{M^2}{s_{23}}\right). \tag{A.6}$$

Here $s \equiv (\mathcal{P}_1 + \mathcal{P}_2)^2$, $t \equiv (\mathcal{K}_2 - \mathcal{P}_2)^2$, $u \equiv (\mathcal{K}_2 - \mathcal{P}_1)^2$, and $s_{ij} \equiv (\mathcal{P}_i + \mathcal{P}_j)^2$; these quantities are related through $s + t + u = s_{12} + s_{13} + s_{23} = M^2$. Setting $M \to 0$ the $2 \to 2$ matrix elements agree with those in ref. [13], with $u \leftrightarrow t$ in the s-channel case.

B   Virtual corrections within the NLO expression

We define a $2 \to 1$ integration measure like in appendix A, but in the presence of dimensional regularization and after the introduction of an infrared regulator λ into the lepton energy:

$$\mathrm{d}\Omega_{2\to 1} \equiv \frac{\mathrm{d}^{3-2\epsilon}\mathbf{p}_1}{2\epsilon_1(2\pi)^{3-2\epsilon}}\frac{\mathrm{d}^{3-2\epsilon}\mathbf{p}_2}{2p_2(2\pi)^{3-2\epsilon}}(2\pi)^{4-2\epsilon}(\mathcal{P}_1 + \mathcal{P}_2 - \mathcal{K}), \tag{B.1}$$

where $\epsilon_1 \equiv \sqrt{p_1^2 + \lambda^2}$ and $\mathcal{P}_1 \equiv (\epsilon_1, \mathbf{p}_1)$. Then the $2 \to 1$ part of the NLO result in eq. (3.4) can formally be written as (for $k_0 > k$)

$$\left[\operatorname{Im}\Pi_{\mathrm{R}}^{\mathrm{NLO}} - \operatorname{Im}\Pi_{\mathrm{R}}^{\mathrm{LO}}\right]_{2\to 1} = \lim_{\lambda\to 0}\int \mathrm{d}\Omega_{2\to 1}\left[1 - n_{\mathrm{F}}(\epsilon_1) + n_{\mathrm{B}}(p_2)\right] \tag{B.2}$$

$$\times \mathbb{P}\Bigg\{m_\ell^2\left[1 + M^2\frac{\overleftarrow{\mathrm{d}}}{\mathrm{d}\lambda^2}\right] - h_t^2 N_{\mathrm{c}}\sum\!\!\!\!\!\!\!\int_{\{Q\}}\frac{M^2}{Q^2(Q - P_2)^2}\bigg|_{p_{2n}=-ip_2}$$

$$+ (g_1^2 + 3g_2^2)\left[-\sum\!\!\!\!\!\!\!\int_{Q}\frac{M^2}{Q^2(Q - K)^2}\bigg|_{k_n=-ik_0} + \sum\!\!\!\!\!\!\!\int_{Q}\frac{M^2}{Q^2(Q - P_2)^2}\bigg|_{p_{2n}=-ip_2}\right.$$

$$+ \sum\!\!\!\!\!\!\!\int_{Q}\frac{M^2 + (1-\epsilon)\,Q \cdot K}{Q^2(Q - P_1)^2}\bigg|_{p_{1n}=-ip_1} + \left.\sum\!\!\!\!\!\!\!\int_{Q}\frac{M^4}{Q^2(Q - P_2)^2(Q - K)^2}\bigg|_{p_{2n}=-ip_2,\, k_n=-ik_0}\right]\Bigg\},$$

where $\mathbb{P}$ refers to a principal value, and $\{Q\}$, P_1 and K are fermionic Matsubara four-momenta (with $P_i \equiv (p_{\mathrm{in}}, \mathbf{p}_i)$ etc). The thermal lepton mass is given by eq. (3.1), and can also be expressed as

$$m_\ell^2 = \frac{g_1^2 + 3g_2^2}{2}\int_{\mathbf{q}}\frac{n_{\mathrm{B}}(q) + n_{\mathrm{F}}(q)}{q}. \tag{B.3}$$

With a similar notation, the LO part can be expressed as (for $m_\phi \to 0$)

$$\lim_{m_\phi\to 0}\operatorname{Im}\Pi_{\mathrm{R}}^{\mathrm{LO}} = M^2\lim_{\lambda\to 0}\int \mathrm{d}\Omega_{2\to 1}\left[1 - n_{\mathrm{F}}(\epsilon_1) + n_{\mathrm{B}}(p_2)\right]. \tag{B.4}$$

Comparing eq. (B.2) with eq. (B.4), most of the terms in eq. (B.2) would appear to be NLO corrections to the LO result. Indeed, evaluating the sum-integrals in the limit of zero temperature and keeping only the $1/\epsilon$-divergences, it can readily be checked that divergences are those cancelled by $\mathcal{Z}_\nu$ of eq. (2.4). However, because momenta are set on-shell in the structures appearing in eq. (B.2), the results are infrared divergent (even at zero temperature). The full result is finite only once summed together with the real processes.

There are a few structures in eq. (B.2) which are particularly important at high temperatures, being of relative magnitude $\sim g^2 T^2/M^2$ in this limit. These are the so-called Hard Thermal Loops (HTLs). Apart from the terms already expressed as m_ℓ^2, the only other HTL originates from $\sum\!\!\!\!\!\!\!\int_Q \frac{Q \cdot K}{Q^2(Q-P_1)^2}$ [23].[5] It turns out, however, that in reality even some non-HTL structures lead to a similarly large final result, despite the apparent prefactor M^2. This issue is discussed in section 6. Here we show that the "normal" HTL structures in eq. (B.2) amount exactly to the HTL resummation of the lepton propagator.

The HTL-resummed inverse lepton propagator reads [28, 29] $\Sigma(P) = i\left[\slashed{P} + \frac{m_\ell^2}{2}\int_\mathbf{v} \frac{i\gamma_0 + \mathbf{v}\cdot\boldsymbol{\gamma}}{ip_n + \mathbf{v}\cdot\mathbf{p}}\right]$, where $|\mathbf{v}| = 1$, $\int_\mathbf{v} 1 = 1$, and we employ Euclidean Dirac-matrices. If the HTL self-energy is treated as an insertion, the lepton propagator reads

$$\Sigma^{-1}(P) = -\frac{i\slashed{P}}{P^2} + \frac{im_\ell^2}{2}\frac{\slashed{P}}{P^2}\int_\mathbf{v} \frac{i\gamma_0 + \mathbf{v}\cdot\boldsymbol{\gamma}}{ip_n + \mathbf{v}\cdot\mathbf{p}}\frac{\slashed{P}}{P^2} \,. \tag{B.5}$$

Determining the correlator of eq. (2.2) with this propagator, we find

$$\Pi_\mathrm{E}^\mathrm{HTL,ins} \equiv \lim_{\lambda\to 0}\int_\mathbf{v}\sum\!\!\!\!\!\!\!\int_P \frac{2}{(P-K)^2}\left\{-\left(1 + m_\ell^2\frac{\mathrm{d}}{\mathrm{d}\lambda^2}\right)\frac{2K\cdot P}{P^2+\lambda^2} - \frac{m_\ell^2\,(ik_n + \mathbf{v}\cdot\mathbf{k})}{(P^2+\lambda^2)(ip_n + \mathbf{v}\cdot\mathbf{p})}\right\}, \tag{B.6}$$

where λ has been introduced as an infrared regulator.

In the last term of eq. (B.6), there are two "inverse propagators", $P^2 + \lambda^2$ and $ip_n + \mathbf{v}\cdot\mathbf{p}$. If the part $P^2 + \lambda^2$ is cut, we get "pole" contributions, whereas cutting $ip_n + \mathbf{v}\cdot\mathbf{p}$ yields a "cut" contribution. These can be separated by partial fractioning ($\epsilon_1 \equiv \sqrt{p^2 + \lambda^2}$),

$$\frac{1}{(P^2+\lambda^2)(ip_n + \mathbf{v}\cdot\mathbf{p})} = \frac{1}{2\epsilon_1}\left[\frac{1}{(\epsilon_1 + \mathbf{v}\cdot\mathbf{p})(\epsilon_1 - ip_n)} - \frac{1}{(\epsilon_1 - \mathbf{v}\cdot\mathbf{p})(\epsilon_1 + ip_n)}\right]$$
$$+ \frac{1}{[\epsilon_1^2 - (\mathbf{v}\cdot\mathbf{p})^2](ip_n + \mathbf{v}\cdot\mathbf{p})} \,. \tag{B.7}$$

The last term represents the soft momentum transfer regime of $2 \leftrightarrow 2$ scatterings, and is analyzed in more detail in appendix C. The structure $1/(\epsilon_1 - ip_n)$ leads to $\delta(k_0 - |\mathbf{p}-\mathbf{k}| + \epsilon_1)$ after carrying out the sum over p_n and taking the cut, which does not get realized for $k_0 > k$. Therefore the only $2 \leftrightarrow 1$ correction arises from the second term of eq. (B.7). Summing this together with the first term in eq. (B.6) and noting that

$$\lim_{\lambda\to 0}\left(1 + m_\ell^2\frac{\mathrm{d}}{\mathrm{d}\lambda^2}\right)(M^2 + \lambda^2)f(\lambda^2) = M^2 f(0) + \lim_{\lambda\to 0}m_\ell^2\left(1 + M^2\frac{\mathrm{d}}{\mathrm{d}\lambda^2}\right)f(\lambda^2)\,, \tag{B.8}$$

the $2 \leftrightarrow 1$ part of eq. (B.6) can be re-written as ($\epsilon_1 \equiv \sqrt{p^2 + \lambda^2}$, $\epsilon_2 \equiv |\mathbf{p}-\mathbf{k}|$)

$$\mathrm{Im}\,\Pi_\mathrm{R}^\mathrm{HTL,ins,pole} \equiv \lim_{\lambda\to 0}\int_{\mathbf{v},\mathbf{p}}\left\{M^2 + m_\ell^2\left(1 + M^2\frac{\mathrm{d}}{\mathrm{d}\lambda^2} - \frac{k_0 + \mathbf{v}\cdot\mathbf{k}}{\epsilon_1 + \mathbf{v}\cdot\mathbf{p}}\right)\right\}$$
$$\times \frac{2\pi\delta(k_0 - \epsilon_1 - \epsilon_2)}{4\epsilon_1\epsilon_2}\left[1 - n_\mathrm{F}(\epsilon_1) + n_\mathrm{B}(\epsilon_2)\right]\,. \tag{B.9}$$

---

[5]Note that terms leading to a thermal Higgs mass were already taken away into eq. (3.2).

It is now easy to check that the m_ℓ^2-parts of eq. (B.9) agree with the HTL parts of eq. (B.2), once the structure $\displaystyle\oint_Q \frac{Q \cdot K}{Q^2 (Q-P_1)^2}\big|_{p_{1n}=-ip_1}$ is expanded to leading order in p_1/T; the thermal lepton mass is identified as eq. (B.3); and a velocity variable is defined as $\mathbf{v} \equiv \mathbf{q}/q$.

C Region of soft momentum transfer

At zero temperature it is well established that infrared (collinear and soft) divergences associated with real and virtual corrections cancel in physical observables. As was observed in refs. [9, 18] (generalizing on a previous analysis at vanishing spatial momentum [30]), a similar cancellation takes place in every "master" spectral function at finite temperature. As a part of the analysis of section 5, we have shown that the cancellation also takes place in the ultrarelativistic regime, where it can be treated within the HTL effective theory (specifically, this refers to the cancellation of λ in eq. (5.9)). In this appendix we provide more details concerning the HTL setup, and also compute the "cut" contributions needed in section 5, representing the effects of $2 \to 2$ scatterings mediated by soft t-channel leptons.

If we consider the correlator of eqs. (2.2), (2.3) within the HTL theory, it may first be verified (by explicit computation) that there is no vertex correction. In the Higgs propagator the only change is the appearance of a thermal mass. Denoting by $\rho_\ell(\omega, \mathbf{p})$ the spectral function corresponding to the lepton propagator, we find

$$\operatorname{Im}\Pi_{\mathrm{R}}^{\mathrm{HTL,full}} \equiv \int_{-\infty}^{\infty}\!\mathrm{d}\omega \int_{\mathbf{p}} \frac{-2\mathcal{K} \cdot \rho_\ell(\omega, \mathbf{p})}{\epsilon_2} \Big[1 - n_{\mathrm{F}}(\omega) + n_{\mathrm{B}}(\epsilon_2)\Big] \delta\big(k_0 - \omega - \epsilon_2\big) \,, \qquad \text{(C.1)}$$

where only that pole from the Higgs propagator which gets realized in practice has been kept, and $\epsilon_2 \equiv \sqrt{(\mathbf{p}-\mathbf{k})^2 + m_\phi^2}$. The spectral function (defined as a four-vector) can be expressed as

$$\rho_\ell(\omega, \mathbf{p}) \equiv \Big(\omega\,\hat{\rho}_0(\omega, p),\, \mathbf{p}\,\hat{\rho}_s(\omega, p)\Big) \,. \qquad \text{(C.2)}$$

Carrying out the angular integral in eq. (C.1) yields

$$\operatorname{Im}\Pi_{\mathrm{R}}^{\mathrm{HTL,full}} = -\frac{1}{2\pi^2 k} \int_{-\infty}^{\infty}\!\mathrm{d}\omega \int_{p_{\min}(\omega)}^{p_{\max}(\omega)} \mathrm{d}p\, p \Big[1 - n_{\mathrm{F}}(\omega) + n_{\mathrm{B}}(k_0 - \omega)\Big]$$

$$\times \left\{ k_0\,\omega\big[\hat{\rho}_0 - \hat{\rho}_s\big] + \frac{M^2 - m_\phi^2 + \omega^2 - p^2}{2}\,\hat{\rho}_s \right\} . \qquad \text{(C.3)}$$

The spectral functions $\hat{\rho}_0, \hat{\rho}_s$ have a "pole part" at $|\omega| > p$ and a "cut part" at $|\omega| < p$. The latter is often referred to as Landau damping, and reflects the effects of $1 \leftrightarrow 2$ scatterings of off-shell leptons on thermal gauge bosons, which are a subpart of $2 \to 2$ scatterings in figure 1. The explicit forms of the spectral functions read

$$\hat{\rho}_0 = \operatorname{Im}\left\{ \frac{1 - \frac{m_\ell^2 L}{2\omega}}{\big[\omega - \frac{m_\ell^2 L}{2}\big]^2 - \big[p + \frac{m_\ell^2(1-\omega L)}{2p}\big]^2} \right\} , \qquad \text{(C.4)}$$

$$\hat{\rho}_s = \operatorname{Im}\left\{ \frac{1 + \frac{m_\ell^2(1-\omega L)}{2p^2}}{\big[\omega - \frac{m_\ell^2 L}{2}\big]^2 - \big[p + \frac{m_\ell^2(1-\omega L)}{2p}\big]^2} \right\} , \qquad \text{(C.5)}$$
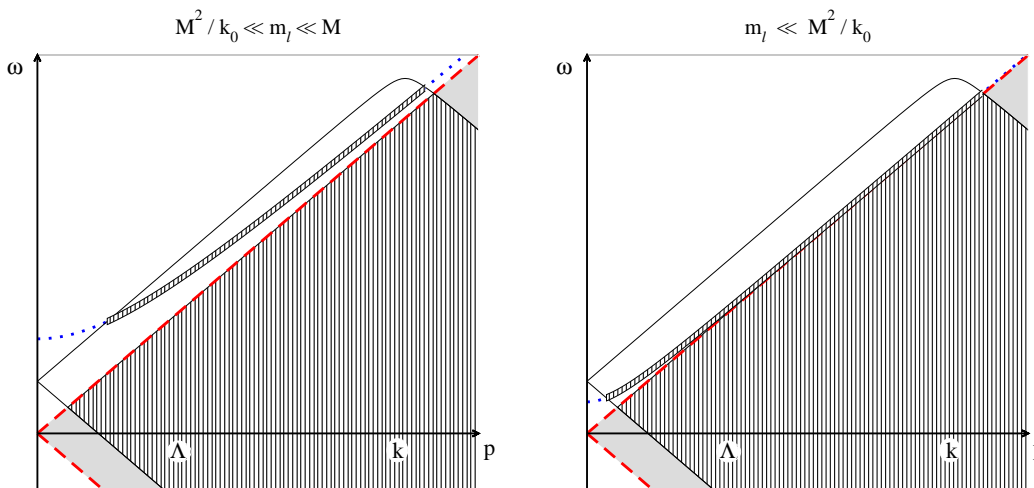
Figure 7. An illustration of the phase space relevant for HTL resummation. The grey-shaded area and the dotted blue line indicate regions in which ρ_ℓ is non-zero (only one pole is shown). The solid black line, with intercept $\omega = k_0 - \sqrt{k^2 + m_\phi^2}$ at $p = 0$, delineates the region allowed kinematically by the δ-constraint in eq. (C.1). The hashed areas denote regions contributing to eq. (C.3).

where $L \equiv \frac{1}{2p} \ln \frac{\omega+p}{\omega-p}$ and ω has a small positive imaginary part. The corresponding phase space is illustrated in figure 7. (There are actually two poles, although only one contributes in the regime $p \gg m_\ell$. Both poles, but no cuts, were included in ref. [31].)

Let us now consider the contribution of soft momenta ($p \lesssim gT$) to $\mathrm{Im}\,\Pi_{\mathrm{R}}^{\mathrm{HTL}}$. For this we introduce a cutoff Λ, satisfying $m_\ell \ll \Lambda \ll k$ (cf. figure 7). In the soft region we can also set $m_\phi = 0$, because the Higgs momentum $\mathbf{k} - \mathbf{p}$ is hard ($p \ll k$); in fact, for the analysis of section 5 we *need* to set $m_\phi = 0$, because this is the case in eq. (3.4). We work within the kinematics relevant for the ultrarelativistic regime, i.e. $M \ll k$, so that $k_0 \approx k$.

In this appendix we focus on soft $2 \to 2$ scatterings which, as mentioned, correspond to the *cut* contribution in the HTL setup. We consider the cut contribution in two different ways. First we consider it in the "full" form as dictated by the HTL theory. Second, we consider it in the "inserted" form in which it appears in the $2 \to 2$ part of the NLO result of section 3, where the scale m_ℓ^2 only appears as an overall prefactor.

For $|\omega| < p$, the function L has an imaginary part, $\mathrm{Im}\,L = -\pi/(2p)$. The cut originates from this imaginary part, and is necessarily proportional to m_ℓ^2. Therefore, omitting higher-order corrections, we can put $M \to 0$ in $p_{\min} = k_- \approx M^2/(4k_0)$. Furthermore, the second term in eq. (C.3) is subleading, given that $\hat{\rho}_s$ is antisymmetric in ω. Therefore the first term gives the leading contribution:

$$
\begin{aligned}
\mathrm{Im}\,\Pi_{\mathrm{R}}^{\mathrm{HTL,full,cut}} &\equiv -\frac{1}{2\pi^2} \int_0^\Lambda \mathrm{d}p\, p \int_{-p}^p \mathrm{d}\omega\, \omega \left[n_{\mathrm{B}}(k_0) + \frac{1}{2} \right] \mathrm{Im} \left\{ \frac{\frac{m_\ell^2(\omega^2 - p^2)L}{2\omega p^2} - \frac{m_\ell^2}{2p^2}}{\left[\omega - \frac{m_\ell^2 L}{2}\right]^2 - \left[p + \frac{m_\ell^2(1-\omega L)}{2p}\right]^2} \right\} \\
&= \frac{m_\ell^2}{4\pi} \left[n_{\mathrm{B}}(k_0) + \frac{1}{2} \right] \left[\ln\left(\frac{2\Lambda}{m_\ell}\right) - 1 \right] + \mathcal{O}\left(\frac{1}{\Lambda}\right) .
\end{aligned}
\tag{C.6}
$$

The integral was carried out by substituting $\omega = px$ whereby the integrations factorize; integrating over p first; expanding the result in powers of m_ℓ^2/Λ^2; and identifying a finite contribution as $\int_{-1}^{+1} \mathrm{d}x\, \mathrm{Im}\left[\left(\frac{1}{2(1-x)} + \frac{1}{4}\ln\frac{1+x}{1-x} - \frac{i\pi}{4}\right) \ln\left(\frac{1}{2(1-x)} + \frac{1}{4}\ln\frac{1+x}{1-x} - \frac{i\pi}{4}\right) \right] = \pi(\ln 2 - 1)$.

(Of course the result is easily reproduced through numerical integration, verifying also that terms argued to be subleading are indeed so.)

Let us now see how the result is modified if we "mistreat" the soft momentum domain by carrying out a Taylor expansion in m_ℓ^2. Expanding eqs. (C.4), (C.5) while keeping $\lambda \equiv 0^+$ as an infrared regulator in the denominator, we have

$$\hat{\rho}_0 \overset{|\omega|<p}{\simeq} \frac{\pi m_\ell^2}{4p\omega(\omega^2 - p^2 - \lambda^2)} \,, \quad \hat{\rho}_s \overset{|\omega|<p}{\simeq} \frac{\pi m_\ell^2 \omega}{4p^3(\omega^2 - p^2 - \lambda^2)} \,. \tag{C.7}$$

Then the inserted cut contribution reads (here the correct integration bounds need to be kept because the infrared domain is not regulated by m_ℓ^2)

$$\mathrm{Im}\,\Pi_{\mathrm{R}}^{\mathrm{HTL,ins,cut}} \equiv -\frac{m_\ell^2}{8\pi} \int_{\frac{M^2}{4k_0}}^{\Lambda} \mathrm{d}p\, p \int_{\frac{M^2}{2k_0}-p}^{p} \mathrm{d}\omega \left[n_{\mathrm{B}}(k_0) + \frac{1}{2} \right] \left\{ -\frac{1}{p^3} + \frac{\omega(M^2 + \omega^2 - p^2)}{2k_0\, p^3(\omega^2 - p^2 - \lambda^2)} \right\}$$

$$= \frac{m_\ell^2}{4\pi} \left[n_{\mathrm{B}}(k_0) + \frac{1}{2} \right] \left[\ln\!\left(\frac{2\Lambda}{\lambda} \right) - 1 \right] + \mathcal{O}\!\left(\frac{1}{\Lambda}, g^4 T^2 \right) \,. \tag{C.8}$$

For completeness we note that the integrand on the first line can also be obtained directly from the last term in eq. (B.7), by taking $\omega \equiv \mathbf{v} \cdot \mathbf{p}$ as an integration variable instead of $\mathbf{v}$.

As expected, eqs. (C.6) and (C.8) depend identically on the ultraviolet cutoff Λ. The dependence on Λ thus cancels in the difference that plays a role in our actual computation, cf. eq. (5.9). In the "fully" HTL-resummed result of eq. (C.6), there is no infrared divergence, with the infrared regime having been regulated by m_ℓ. In the "inserted" HTL result of eq. (C.8), there is an infrared divergence, but this cancels against a corresponding divergence in the inserted pole contribution, as is demonstrated in eq. (5.9). This cancellation completes the proof of infrared insensitivity of the observable $\mathrm{Im}\,\Pi_{\mathrm{R}}$ within the HTL setup.

D   Choice of parameters

The physical Higgs mass is set to $m_H = 126\,\mathrm{GeV}$. In order to convert pole masses and the muon decay constant to $\overline{\mathrm{MS}}$ scheme parameters at a scale $\bar{\mu} = \bar{\mu}_0 \equiv m_Z$ we employ 1-loop relations specified in ref. [32]; subsequently, 1-loop renormalization group equations determine the running of the couplings to a scale

$$\bar{\mu}_{\mathrm{ref}} \equiv \max(M, \pi T) \,, \tag{D.1}$$

where they are evaluated for purposes of the present paper. Within this approximation the U(1), SU(2) and SU(3) gauge couplings g_1^2, g_2^2, g_3^2 have explicit solutions (we have set $N_c = 3$ and considered 3 families),

$$g_1^2(\bar{\mu}) = \frac{48\pi^2}{41\ln(\Lambda_1/\bar{\mu})} \,, \quad g_2^2(\bar{\mu}) = \frac{48\pi^2}{19\ln(\bar{\mu}/\Lambda_2)} \,, \quad g_3^2(\bar{\mu}) = \frac{24\pi^2}{21\ln(\bar{\mu}/\Lambda_3)} \,, \tag{D.2}$$

where $\Lambda_1, \Lambda_2, \Lambda_3$ are solved from the boundary values at $\bar{\mu} = \bar{\mu}_0$. The top Yukawa and the Higgs self-coupling at $\bar{\mu} > \bar{\mu}_0$ are solved numerically from

$$\bar{\mu}\frac{\mathrm{d}h_t^2}{\mathrm{d}\bar{\mu}} = \frac{h_t^2}{8\pi^2} \left[\frac{9}{2}h_t^2 - \frac{17}{12}g_1^2 - \frac{9}{4}g_2^2 - 8g_3^2 \right] \,, \tag{D.3}$$

$$\bar{\mu}\frac{\mathrm{d}\lambda}{\mathrm{d}\bar{\mu}} = \frac{1}{8\pi^2} \left[\frac{3}{16}\left(g_1^4 + 2g_1^2 g_2^2 + 3g_2^4 \right) - \frac{3}{2}\lambda\left(g_1^2 + 3g_2^2 \right) + 12\lambda^2 + 6\lambda h_t^2 - 3h_t^4 \right] \,. \tag{D.4}$$

For definiteness let us recall that at tree level $\lambda \approx g_2^2 m_H^2/(8m_W^2) \approx 0.13$.

References

[1] M. Fukugita and T. Yanagida, *Baryogenesis Without Grand Unification*, *Phys. Lett.* **B 174** (1986) 45 [INSPIRE].

[2] S. Davidson, E. Nardi and Y. Nir, *Leptogenesis*, *Phys. Rept.* **466** (2008) 105 [arXiv:0802.2962] [INSPIRE].

[3] X. Shi and G.M. Fuller, *A new dark matter candidate: Nonthermal sterile neutrinos*, *Phys. Rev. Lett.* **82** (1999) 2832 [astro-ph/9810076] [INSPIRE].

[4] L. Canetti, M. Drewes, T. Frossard and M. Shaposhnikov, *Dark Matter, Baryogenesis and Neutrino Oscillations from Right Handed Neutrinos*, *Phys. Rev.* **D 87** (2013) 093006 [arXiv:1208.4607] [INSPIRE].

[5] A. Salvio, P. Lodone and A. Strumia, *Towards leptogenesis at NLO: the right-handed neutrino interaction rate*, *JHEP* **08** (2011) 116 [arXiv:1106.2814] [INSPIRE].

[6] M. Laine and Y. Schröder, *Thermal right-handed neutrino production rate in the non-relativistic regime*, *JHEP* **02** (2012) 068 [arXiv:1112.1205] [INSPIRE].

[7] S. Biondini, N. Brambilla, M.A. Escobedo and A. Vairo, *An effective field theory for non-relativistic Majorana neutrinos*, *JHEP* **12** (2013) 028 [arXiv:1307.7680] [INSPIRE].

[8] S. Caron-Huot, *Asymptotics of thermal spectral functions*, *Phys. Rev.* **D 79** (2009) 125009 [arXiv:0903.3958] [INSPIRE].

[9] M. Laine, *Thermal right-handed neutrino production rate in the relativistic regime*, *JHEP* **08** (2013) 138 [arXiv:1307.4909] [INSPIRE].

[10] D. Bödeker and M. Wörmann, *Non-relativistic leptogenesis*, *JCAP* **02** (2014) 016 [arXiv:1311.2593] [INSPIRE].

[11] D. Besak and D. Bödeker, *Hard Thermal Loops for Soft or Collinear External Momenta*, *JHEP* **05** (2010) 007 [arXiv:1002.0022] [INSPIRE].

[12] A. Anisimov, D. Besak and D. Bödeker, *Thermal production of relativistic Majorana neutrinos: Strong enhancement by multiple soft scattering*, *JCAP* **03** (2011) 042 [arXiv:1012.3784] [INSPIRE].

[13] D. Besak and D. Bödeker, *Thermal production of ultrarelativistic right-handed neutrinos: Complete leading-order results*, *JCAP* **03** (2012) 029 [arXiv:1202.1288] [INSPIRE].

[14] B. Garbrecht, F. Glowna and P. Schwaller, *Scattering Rates For Leptogenesis: Damping of Lepton Flavour Coherence and Production of Singlet Neutrinos*, *Nucl. Phys.* **B 877** (2013) 1 [arXiv:1303.5498] [INSPIRE].

[15] D. Bödeker and M. Laine, *Kubo relations and radiative corrections for lepton number washout*, *JCAP* **05** (2014) 041 [arXiv:1403.2755] [INSPIRE].

[16] B. Garbrecht, F. Glowna and M. Herranen, *Right-Handed Neutrino Production at Finite Temperature: Radiative Corrections, Soft and Collinear Divergences*, *JHEP* **04** (2013) 099 [arXiv:1302.0743] [INSPIRE].

[17] S. Caron-Huot, *On supersymmetry at finite temperature*, *Phys. Rev.* **D 79** (2009) 125002 [arXiv:0808.0155] [INSPIRE].

[18] M. Laine, *Thermal 2-loop master spectral function at finite momentum*, *JHEP* **05** (2013) 083 [arXiv:1304.0202] [INSPIRE].

[19] J. Frenkel and J.C. Taylor, *Hard thermal QCD, forward scattering and effective actions*, *Nucl. Phys.* **B 374** (1992) 156 [INSPIRE].

[20] E. Braaten and R.D. Pisarski, *Simple effective Lagrangian for hard thermal loops*, *Phys. Rev.* **D 45** (1992) 1827 [INSPIRE].

[21] I. Ghisoiu and M. Laine, *Interpolation of hard and soft dilepton rates*, *JHEP* **10** (2014) 083 [`arXiv:1407.7955`] [InSPIRE].

[22] M.J. Strassler and M.E. Peskin, *Threshold production of heavy top quarks: QCD and the Higgs boson*, *Phys. Rev.* **D 43** (1991) 1500 [InSPIRE].

[23] E. Braaten and R.D. Pisarski, *Soft Amplitudes in Hot Gauge Theories: A General Analysis*, *Nucl. Phys.* **B 337** (1990) 569 [InSPIRE].

[24] J. Ghiglieri, J. Hong, A. Kurkela, E. Lu, G.D. Moore and D. Teaney, *Next-to-leading order thermal photon production in a weakly coupled quark-gluon plasma*, *JHEP* **05** (2013) 010 [`arXiv:1302.5970`] [InSPIRE].

[25] J. Ghiglieri and G.D. Moore, *Low Mass Thermal Dilepton Production at NLO in a Weakly Coupled Quark-Gluon Plasma*, `arXiv:1410.4203` [InSPIRE].

[26] M. D'Onofrio, K. Rummukainen and A. Tranberg, *The Sphaleron Rate in the Minimal Standard Model*, *Phys. Rev. Lett.* **113** (2014) 141602 [`arXiv:1404.3565`] [InSPIRE].

[27] T. Asaka, M. Laine and M. Shaposhnikov, *Lightest sterile neutrino abundance within the νMSM*, *JHEP* **01** (2007) 091 [`hep-ph/0612182`] [InSPIRE].

[28] V.V. Klimov, *Collective Excitations in a Hot Quark Gluon Plasma*, *Sov. Phys. JETP* **55** (1982) 199 [*Zh. Eksp. Teor. Fiz.* **82** (1982) 336] [InSPIRE].

[29] H.A. Weldon, *Effective fermion masses of order gT in high temperature gauge theories with exact chiral invariance*, *Phys. Rev.* **D 26** (1982) 2789 [InSPIRE].

[30] M. Laine, A. Vuorinen and Y. Zhu, *Next-to-leading order thermal spectral functions in the perturbative domain*, *JHEP* **09** (2011) 084 [`arXiv:1108.1259`] [InSPIRE].

[31] C.P. Kiessig, M. Plümacher and M.H. Thoma, *Decay of a Yukawa fermion at finite temperature and applications to leptogenesis*, *Phys. Rev.* **D 82** (2010) 036007 [`arXiv:1003.3016`] [InSPIRE].

[32] K. Kajantie, M. Laine, K. Rummukainen and M.E. Shaposhnikov, *Generic rules for high temperature dimensional reduction and their application to the standard model*, *Nucl. Phys.* **B 458** (1996) 90 [`hep-ph/9508379`] [InSPIRE].